Available online at www.sciencedirect.com
SCIENCE DIRECT®
International Journal of Heat and Fluid Flow 26 (2005) 25–33
International Journal of HEAT AND FLUID FLOW
www.elsevier.com/locate/ijhff

Effect of the gap size in the start-up free convective flow around a square prism near a wall

Stéphane Fohanno *, Guillaume Polidori

Laboratoire de Thermomécanique, BP 1039, Moulin de la Housse, 51687 Reims Cedex 2, France

Received 25 July 2003; accepted 19 June 2004
Available online 11 September 2004

Abstract

Flow visualizations and thermal measurements have been employed to analyse the transient free convective flow in the vicinity of a square prism ($D \times 2D \times 2D$) near a vertical heated wall for a modified Rayleigh number $Ra^* < 4.5 \times 10^{10}$. The effect of changing the gap, G, between the prism and the wall from $G = 0$ (prism touching the wall) to $G \to \infty$ (no prism at all) was investigated. It is shown that the reduction of the gap height $G/D \leqslant 0.1$ results in more complex flow patterns due to the increase of the adverse pressure gradient leading to the separation of the viscous layer downstream of the prism. Consequently, as well enhancement ($G/D = 0$) as degradation ($G/D = 0.1$) in the heat transfer performance occur in the prism wake. These phenomena are more pronounced in the early start-up of the flow.

1. Introduction

This work focusses on an experimental investigation of the transient laminar free convective flow around a short square prism placed in the proximity of a wall boundary layer for several gap-to-prism height ratios. The understanding gained from the study of this geometry is relevant to several practical applications such as electronics industry where components are not necessarily pinned to the wall.

When located in an on-coming stream, obstacles induce complex flow patterns with regions of flow separation, reattachment and recirculation. It is known that the presence of the obstruction leads to a substantial change in the heat transfer rate as compared with the unobstructed flow. Nevertheless, the mechanism leading to heat transfer enhancement due to vortex separation is still poorly understood and results are somewhat contradictory in literature for free convection flows.

Aydin (1997) showed that the presence of transverse roughness elements can slightly increase heat transfer when ribs have a poor thermal conductivity. Lin and Hsieh (1990) concluded that the existence of protruding 2D-ribs at the wall originates a flow separation/recirculation which is one of the major factors influencing the local temperature gradients. Burak et al. (1995) studied the case of a vertical heated plate in the presence of one or several rectangular steps and evidenced from flow visualization a rotational flow between the ribs which intensifies the process of heat transfer. On the contrary, considering an array of heated protrusions on a vertical surface in water, Joshi et al. (1989) presented flow visualizations with no evidence of vortex formation around the protrusions. Shakerin et al. (1988) have observed that the influence of the roughness is mainly localized to within about two roughness heights above and below the roughness location. Nevertheless, they have not observed from dye visualization the presence of a flow-separation bubble inside the cavities between the ribs. Polidori and Padet (2003) concluded that during the early transient an important heat transfer enhancement

* Corresponding author. Tel./fax: +33 326 91 83 10.
E-mail address: stephane.fohanno@univ-reims.fr (S. Fohanno).

0142-727X/$ - see front matter © 2004 Elsevier Inc. All rights reserved.
doi:10.1016/j.ijheatfluidflow.2004.06.004

Nomenclature

D	thickness of the prism (D = 20 mm)
g	acceleration of gravity, ms^{-2}
G	gap height, m
h	convective heat transfer coefficient, $Wm^{-2}K^{-1}$
h_0	convective heat transfer coefficient for the smooth case, $Wm^{-2}K^{-1}$
Pr	Prandtl number
Ra	Rayleigh number, $= Pr\, g\beta(T_w - T_\infty)x^3/\nu^2$
Ra^*	modified Rayleigh number, $= Pr\, g\beta\varphi_w x^4/\lambda\nu^2$
t	time, s
T_w	wall temperature, K
T_∞	ambient temperature, K
T_P	prism surface temperature, K
U	velocity profile, ms^{-1}
x, y	Cartesian coordinates, m
Greeks	
β	coefficient of thermal expansion, K^{-1}
δ	dynamic boundary layer thickness, m
φ_w	heat flux density, Wm^{-2}
λ	thermal conductivity, $Wm^{-1}K^{-1}$
ν	kinematic viscosity, m^2s^{-1}
Δ	thermal to dynamic boundary layer thickness ratio (Δ = 0.653 for Pr = 7)

occurs in the upstream part of the cavity between the ribs while increasing time reduces the heat transfer performance in the whole cavity due to complex eddy structures. Acharya and Mehrotra (1993) indicated that a smooth surface yields a greater heat transfer rate when compared with ribbed geometries due to dead regions in the near-rib space. Tanda (1997) has shown that the presence of ribs was found to alter the heat transfer considerably causing thermally inactive regions just upstream and downstream of each protrusion. Vermeulen (1997) also found that in the vortical region above the rib, the convective heat transfer coefficient is lower than those in any other region. Focussing attention on the surface geometry, Bhavnani and Bergles (1990) specified that ribbed surfaces resulted in degraded heat transfer performance while stepped geometries can be used in general to improve the heat transfer. Desrayaud and Fichera (2002) have specified in the case of a channel that increasing the length of the rib has only a limited influence on the heat transfer while increasing its width decreases dramatically the heat transfer. Abu-Mulaweh et al. (1995) also found for natural convection flow over a backward-facing step that heat transfer coefficients decrease with increasing the step height. Focussing attention on the angular position of prism within the on-coming boundary layer, Polidori et al. (2002) concluded that small angle values lead to heat transfer enhancement in the early transient.

Thus much literature on the subject is dedicated to the study of flow around two-dimensional or three-dimensional-shape protrusions mounted on a vertical surface. Although the fluid dynamics is now reasonably studied when the prism is positioned close to a plane wall boundary in adiabatic thermal situation (a summary of works is reviewed in Price et al., 2002) or in forced convection (Rampanarivo, 2000), this is not the case in free thermal convection. The current investigation is, to the knowledge of the authors, the first to document both the unsteady heat transfer and flow features over a bluff-body suspended in a free convection on-coming boundary layer.

To get a better fundamental understanding of such a separation flow and how it can interact with the on-coming boundary layer, a square prism whose height is D was detached from the wall so that its influence on the free convection flow was characterized by several G-gap heights in the range $0 \leqslant G/D \leqslant \infty$. To facilitate the understanding of the physics, visualization experiments were used to qualitatively document the flow field behaviour while thermocouples were located at the wall.

2. Experimental apparatus and methodology

2.1. Water tank and heating wall/prism system

Two different experimental investigations were performed to access both heat transfer and flow patterns. All thermal measurements and flow visualizations were made in a 50 cm × 50 cm × 100 cm deep tank filled with water and having 20 mm thick Plexiglas® walls. A vertical wall dissipating a uniform heat flux was used to generate a buoyancy induced flow in water. This thermal system (Fig. 1) consists of a vertical plane thermofoil heater (20×30 cm^2) delivering a uniform heat flux density (3300 W/m^2) insulated on one side and covered with a 300 μm thin steel plate on the other side. To ensure the thermal condition, the uniform heat flux condition has been controlled from the measurement of the wall temperature distribution indicating that $(T_w - T_\infty)$ does indeed vary downstream as $x^{0.2}$. This gave a flux based Rayleigh number (Ra^*) such that $Ra^* < 4.5\times10^{10}$ which corresponds to a domain of laminar convection flow in water. Indeed, it is generally accepted that the position

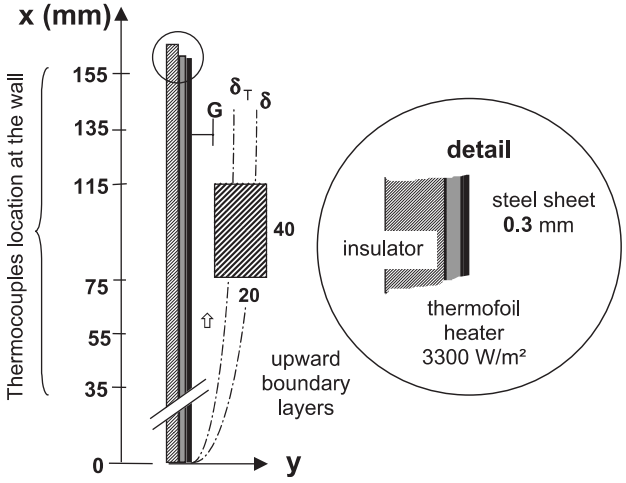

Fig. 1. Schematic sketch of the experimental arrangement.

of transition from the laminar to the turbulent regime in water occurs in the range $3\times10^{12} < Ra^* < 10^{14}$ for the uniform heat flux heating problem in free convection along a vertical wall (Vliet and Liu, 1969) while this transition occurs somewhere about $2\times10^{9} < Ra < 5\times10^{9}$ in water and air (Tsuji and Nagano, 1988a,b, 1989) for the constant temperature heating problem.

A Plexiglas square prism ($40\times40\times20$ mm^3) with the upstream cylinder face normal to the main free convection flow has been used to disturb the boundary layer growth. Its reference height is noted D ($D = 20$ mm). The square geometry is convenient because it is a simple bluff-body for which the separation points are fixed, unlike the case of circular cylinders. This prism was thermally quasi-passive ($\lambda = 0.26$ W/mK) to avoid conduction paths within it. Before starting any experimental run, the water was stirred to ensure temperature uniformity. After the fluid was quiescent, the wall was impulsively subjected to a uniform heat flux generating the unsteady behaviour of the free convection flow.

All the thermocouples used in the instrumentation were chromel-alumel type gauges, calibrated to ±0.1 K. These thermocouples were placed along the vertical centre line of the wall/prism system at six different locations as indicated in Fig. 1. Three of them were located upstream of the prism ($x = 35, 55, 75$ mm) while the other ones were located downstream of the prism ($x = 115, 135, 155$ mm); the thermocouples were regularly spaced at intervals of $D = 20$ mm. No thermocouple was located between the wall and the prism to avoid any disturbance in the fluid motion. The thermocouples were sticked on the water side of the vertical wall and a special attention has been made with the surface gluing process in order to avoid the insertion of a thermal resistance between the wall and the gauge. These gauges are then connected to a data logger (*AOIP Instruments PC10*) whose acquisition is every 3 s.

2.2. Boundary layer prediction close to the wall

The prism was positioned close to the plate 75 mm from the leading edge of the plate, see Fig. 1. Because the effect of changing the gap G/D between the prism and the wall was the main parameter of this experimental analysis, preliminary knowledge of the prism location compared to the inherent thermal and dynamic boundary layer thicknesses was necessary. So, to precise the scene of the study we have considered the smooth wall case without the presence of the square cylinder from a theoretical viewpoint. Therefore, assuming a laminar boundary layer on the plane wall, the dynamic and thermal fields (1) are estimated from an integral approach (Kakaç and Yener, 1995) as

$$\begin{cases} U = \frac{g\beta\varphi_w\Delta\delta^3}{12\lambda\nu}\left[-\eta^4+3\eta^3-3\eta^2+\eta\right] \\ \Theta = T - T_\infty = \frac{\varphi_w\Delta\delta}{2\lambda}\left[-\eta_T^4+2\eta_T^3-2\eta_T+1\right] \end{cases} \quad (1)$$

with $\eta = \frac{y}{\delta} \leqslant 1$, $\eta_T = \frac{y}{\delta_T} \leqslant 1$. The dynamic boundary layer thickness is analytically deduced from the resolution of the governing conservation equations as the asymptotical steady limit of the transient (Polidori et al., 2000) and expressed as

$$\delta(x) = \left[\frac{432\lambda\nu^2}{g\beta\varphi_w\Delta}(9\Delta-5)x\right]^{\frac{1}{5}}. \quad (2)$$

where Δ is the thermal to hydrodynamic boundary layer thickness ratio estimated from the von Karman-Pohlhausen integral method extended to the general case with no assumption of a common boundary layer thickness (Mladin et al., 1999) for both temperature and velocity. Δ is numerically found to be 0.653 for $Pr = 7$.

Applying (2) gives the on-coming viscous boundary layer thickness to be 5.6 mm at the vertical location of the cylinder without the presence of the cylinder. Both boundary layer thicknesses and the temperature and velocity profiles at the prism location are reported in Fig. 2. The different chosen gaps between the prism

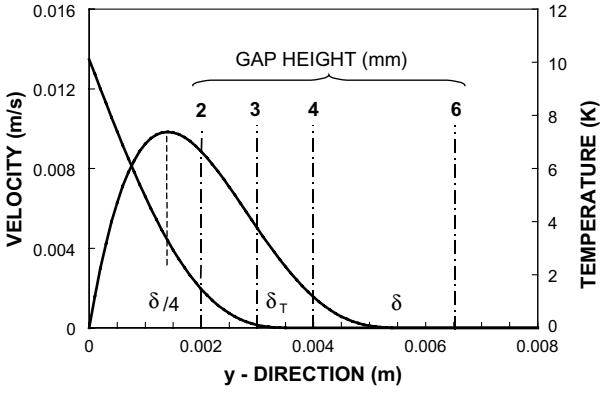

Fig. 2. Prism location within the free convection boundary layers.

and the wall ($2 \leqslant G \leqslant 6$ mm or $0.1 \leqslant G/D \leqslant 0.3$) are also mentioned.

2.3. Flow visualization experiments

The flow was illuminated by a *Coherent*® model laser tuned to 514.5 nm at which its rated power is about 2 W, coupled with a sphero-cylindrical optical device to generate a laser sheet in the plane of symmetry of the prism. To allow the time-evolution of the flow, the analysis was made in the vicinity of the obstacle by means of the solid tracer visualization technique. Lighted particles of Rilsan® with average particle diameter of 100 μm, correctly seeded inside the tank, were recorded with a suitable time of exposure to obtain instantaneous streak fields which, after analysis, enables one to precisely identify streamline patterns and to deduce topological critical points (Hunt et al., 1978) as well as streamline patterns. In the experiments, flow development is sequentially recorded by a digital camera (*Olympus*® C-2500L) with an exposure time of 2 s fitted to the low flow velocities and unsteady phenomena occurring in such free convection flows; the acquisition is then coupled with a computer for data analysis.

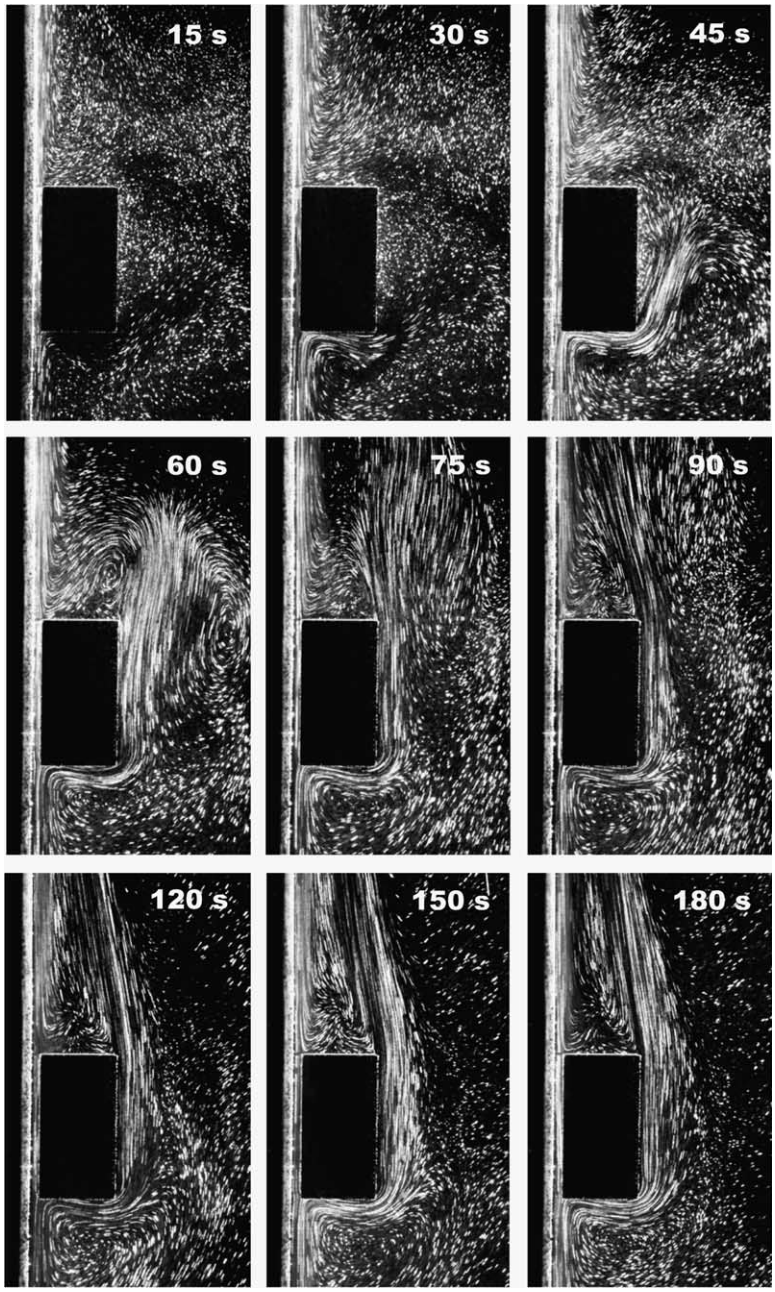

Fig. 3. Flow development around the square prism for a 2 mm gap height.

3. Results and discussion

3.1. General description of the start-up flow

Examples of flow visualizations of the free convection flow growth on the vertical plate with a uniform heat flux in the presence of the prism are presented in Fig. 3. The fluid motion is from bottom to top and the gap size is fixed to 2 mm ($G/D = 0.1$) with sequences every 15 or 30 s up to $t = 180$ s. As it can be seen after the start of the heating process, the presence of the prism near the wall causes the separation of the dynamic boundary layer. Consequently, two oppositely rotating vortices are observed in the separation region directly near the prism ($t = 45$ and 60 s). One of them vanishes before to be shed downstream while the other one feeds the near-wake recirculation flow. Increasing time leads to no change in the near-wake shape where a highly three-dimensional behaviour occurs.

To document as well mean flow structures as vortical features of the near-wake formation, evolution in time of detailed instantaneous streamline patterns are presented in Fig. 4 up to time $t = 120$ s, corresponding to a quasi-steady dynamic state from which no significant modification in the fluid dynamics is observed.

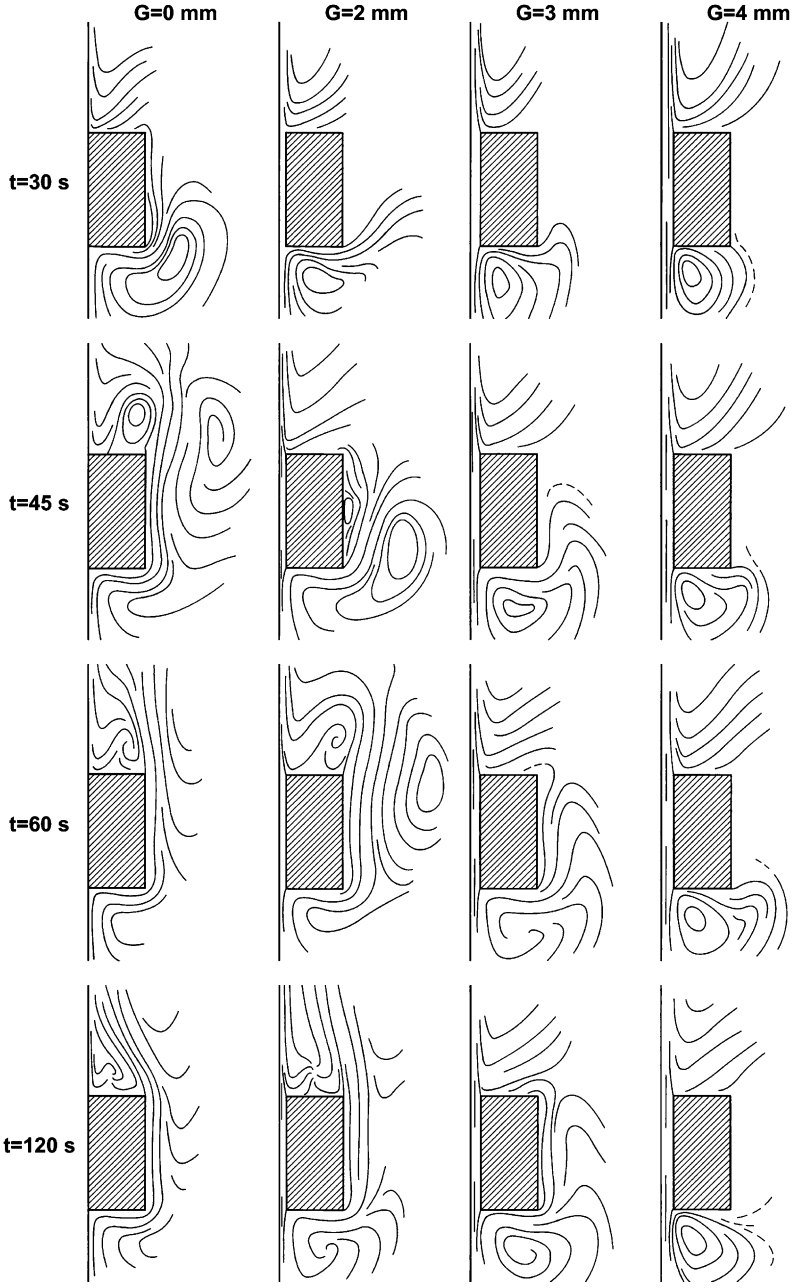

Fig. 4. Streamline patterns in the vicinity of the prism.

Because the flow structures are highly sensitive to small gap heights, comparisons are made for four different gap sizes, from $G = 0$ (prism at the wall) to $G = 4$ mm ($G/D = 0.2$). The case $G = 6$ mm ($G/D = 0.3$) is not presented because it induces no significant modification in the flow behaviour in comparison with the smooth case ($G/D \to \infty$). The reason is that the prism is no longer within the dynamic boundary layer, confirming the previous theoretical results on the dynamic layer thickness, found to be $\delta = 5.6$ mm at the prism location.

Whatever the gap size, it can be observed that the pressure field created by the prism is not sufficient in the free convection to make the boundary layer separate upstream the field like in forced convection (horse-shoe type vortex). Nevertheless, the blockage effect results in a upstream primary vortical structure below the prism whose feature and time-evolution change significantly as a function of the gap height.

When $G \geqslant 4$ mm ($G/D \geqslant 0.2$), there is no fluid motion around the prism. The on-coming fluid mainly flows between the wall and the prism. Nevertheless, due to the prim obstruction, external part of the boundary layer rolls up into a vortex remaining confined below the prism into a two-dimensional shape. For $G = 3$ mm ($G/D = 0.15$), the on-coming boundary layer turns around the prism but the resulting pressure gradient is not sufficient to make the flow separate at the prism trailing edges. Consequently, one observes no vortex formation above the prism. For $G = 0$ or 2 mm ($G/D \leqslant 0.1$), the blockage effect is sufficient to create a pressure gradient responsible for the separation of the boundary layer into a three-dimensional near-wake downstream of the prism.

3.2. Transient heat transfer

To assist in analyzing the influence of the gap height on the heat transfer performance in the vicinity of the prism, temperature measurements have been performed along the wall.

First, in order to assess the validity of the assumption of using a thermally quasi-passive obstacle and to verify that the residual conduction within the prism generated from the heated wall is not sufficient to affect the heat transfer at the fluid/prism interface, specific temperature measurements at the prism surface have also been carried out. Three particular locations at the centre of the lower, front and upper faces of the obstacle have been chosen due to their relevance with respect to the main flow wise around the obstacle as shown in Fig. 5. Corresponding thermal measurements are presented in Fig. 6, respectively for $G/D = 0$ and 0.1, which are the situations where the effects of conduction, if any, should be the most significant. Whatever the gap size, the main

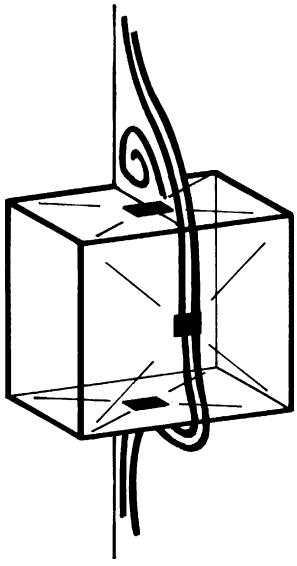

Fig. 5. Sketch of the flow around the prism with locations of the temperature measurements on the prism (black rectangles).

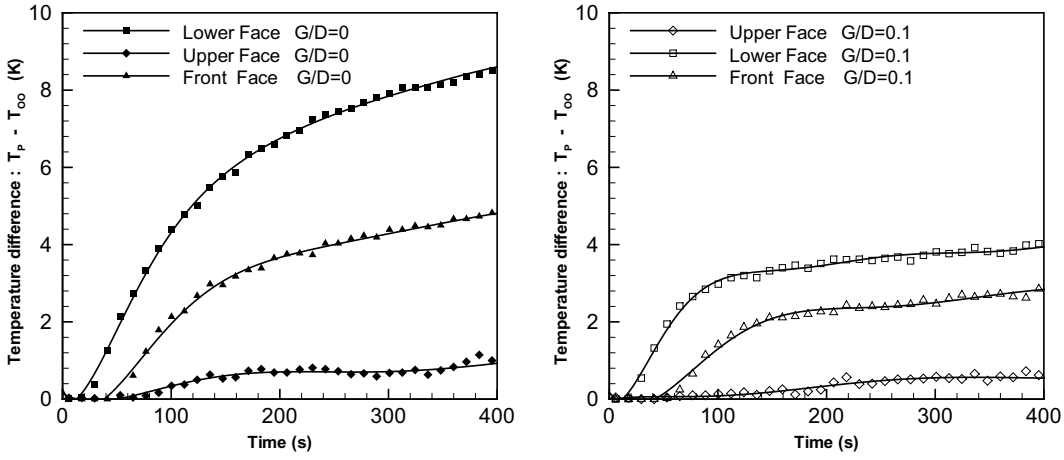

Fig. 6. Time-evolution of the surface temperatures of the lower, front and upper faces of the prism for $G/D = 0$ (left) and $G/D = 0.1$ (right).

conclusions are that, despite analogous locations from the wall in the lower and the upper surface temperature measurements, drastic differences appear showing that interfacial thermal phenomena are mainly governed by the effects of convection. This is confirmed by the curve layout showing the fluid blockage effect at the lower face of the prism leading to a higher temperature increase. Then, a decrease in the interfacial temperature is observed downstream of this first location due to the fluid flowing in contact with the quasi-passive obstacle, in agreement with the topological fluid behaviour presented in Fig. 4. Moreover, the temporal delays observed in the start of the temperature time-evolution are similar to those observed from the visualizations of the convective flow establishment in Fig. 3. Furthermore, one can ensure that the effect of conduction within the prism on the interfacial heat transfer characteristics is negligible compared to that of convection from the analysis of the two plots related to the upper face temperatures for $G/D = 0$ where the prism is at the wall and $G/D = 0.1$. The evolutions are found to be similar with only an initial time-delay for the $G/D = 0.1$ case also confirmed in the flow topological features given in Fig. 4.

Dimensionless heat transfer results for the convection flow in presence of the prism are presented in Fig. 7 and Fig. 8. To access to the h convective heat transfer coefficient one extends to the transient the Newton's law:

$$h(x,t) = \frac{\varphi_w}{T_w(x,t) - T_\infty} \tag{3}$$

The experimental thermal uncertainties have been fully described and discussed previously in Polidori and Padet (2003) and only the resulting formulation found to be pertinent with these specific experiments is given as

$$\frac{\Omega(h)}{h} \approx \frac{9}{4}\frac{\Omega(T_w) + \Omega(T_\infty)}{|\,T_w - T_\infty\,|} \tag{4}$$

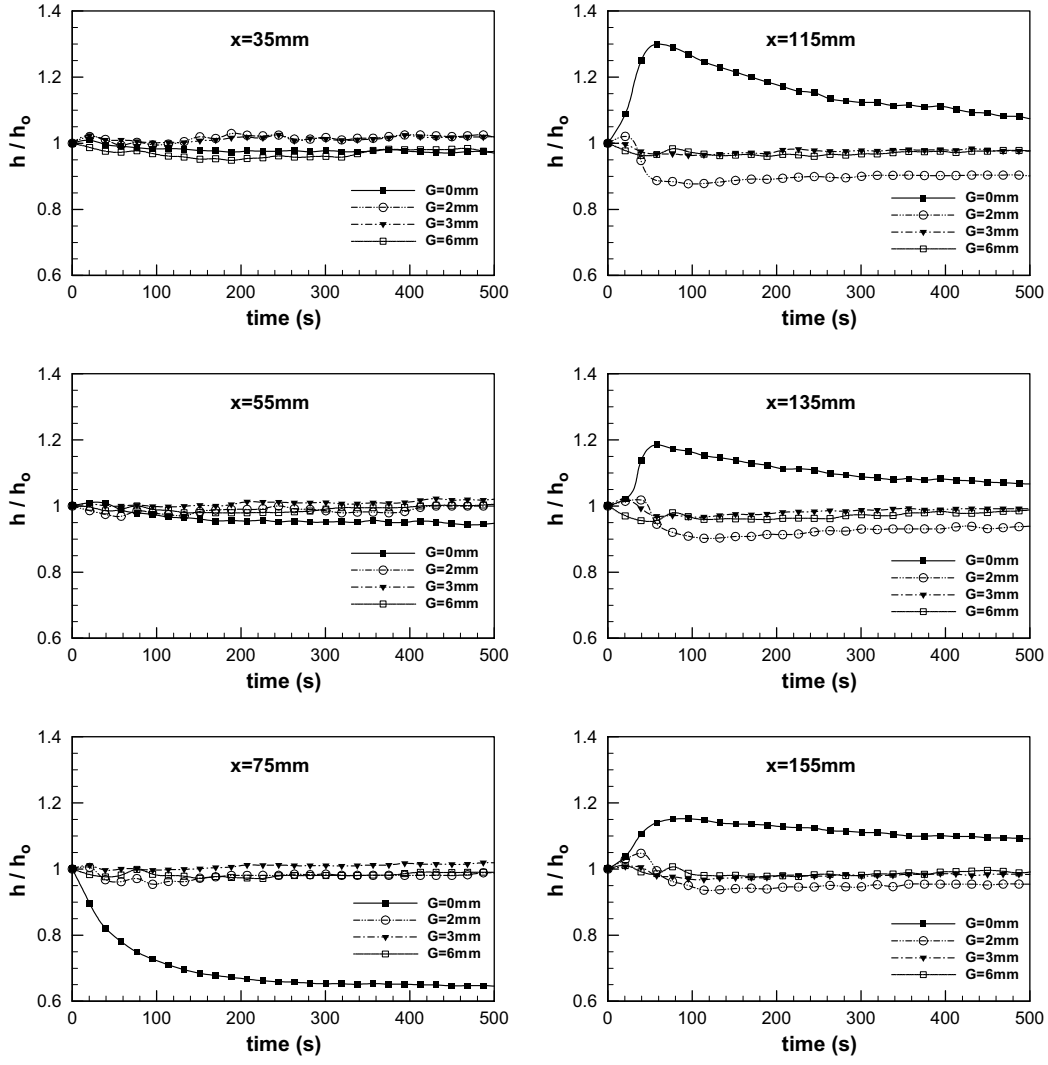

Fig. 7. Time-evolution of heat transfer along the plate.

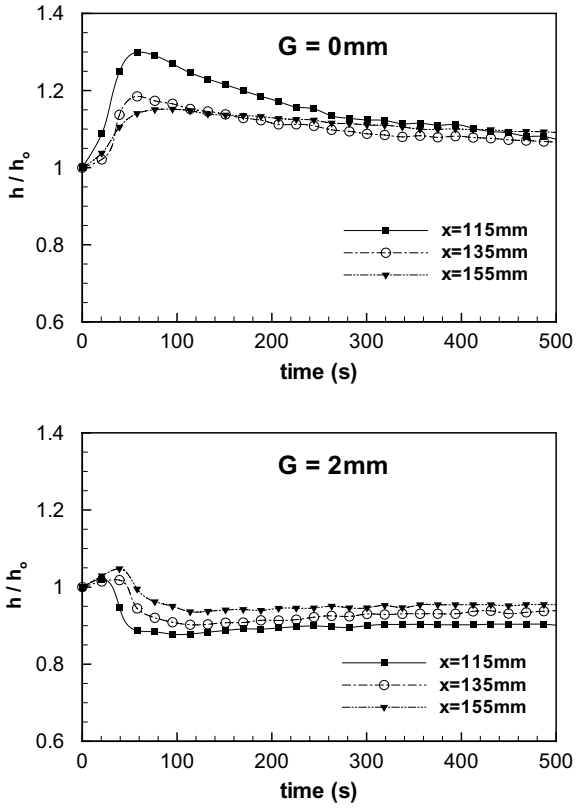

Fig. 8. Heat transfer evolution downstream of the prism for small gaps.

where $\Omega(\ )$ is the absolute uncertainty of the parameter $(\ )$. Consequently, these uncertainties in the heat transfer coefficient are estimated to be within ±4.5%.

Of particular interest is the comparison depicted in Fig. 7 where the ratio between local heat transfer coefficients pertaining to the "rough" and smooth plate $h(x,t)/h_0(x,t)$ is plotted as a function of time. One observes that the influence of the prism is mainly localized to within about one prism height below and more than two D-heights above the prism location. Just below the prism and increasing time, the heat transfer performance of the prism mounted wall ($G = 0$) turns out to be about 35% lower than that of the corresponding smooth wall. This is in good agreement with conclusions of Polidori and Padet (2003) on a vertical surface with an array of large-scale roughness elements. Moreover, upstream of the flow, the gap between the wall and the prism does not seem to be a significant parameter which affects the heat transfer.

On the contrary, the results are more contrasted downstream of the prism (x = 115–155 mm). The blockage effect plays an important role on the local heat transfer performance.

For $G = 0$, a peak in the curves of heat transfer enhancement is observed in the early transient. This peak is all the more marked (up to 30%) that the measurement is close to the prism. Increasing time leads to a decrease of the heat transfer enhancement. For $G = 2$ mm ($G/D = 0.1$), a degradation in the heat transfer performance occurs. Nevertheless, in the start-up transient, one observes an extremum in the curves with an enhancement tendency before tending to a degradation in heat transfer up to about 10%. The physical reason of degradation seems to be the decrease of the fluid velocity between the wall and the prism leading to an increase of the temperature at the wall compared to the smooth case.

For both previous cases, the curves tendency is to reach a steady heat transfer behaviour with increasing time.

For gap-sizes such that $G/D \geqslant 0.15$, the blockage effect ratio is not sufficient to induce any modification in the local heat transfer downstream of the prism.

A close-up view of these results is shown in Fig. 8 where the heat transfer evolution for the cases $G = 0$ and 2 mm ($G/D = 0.1$) is reported. These results show that the more significant modifications in the heat transfer performance occur in the early start-up of the free convection flow up to $t = 200$ s for $G = 0$ and $t = 100$ s for $G = 2$ mm.

4. Conclusion

From the authors knowledge, free convection flow over suspended obstacles had not yet been studied in free convection. Thus, the development in time of natural convection from a uniformly heated vertical wall in presence of a three dimensional square cylinder mounted in the vicinity of a solid wall is studied experimentally. The influence of the gap height on the development of the on-coming boundary layer was analysed from both heat transfer and dynamic viewpoints.

Based on these data, the main following conclusions can be drawn:

1. In the early transient, a upstream primary vortical structure is forming below the prism as a result of the blockage effect. Its feature and time-evolution change significantly as a function of the gap height. For $G/D \leqslant 0.1$, larger blockage effects result in higher velocity in the separated viscous layer leading to a near wake formation downstream of the prism while for larger gap heights the downstream vortex formation does not occur.
2. During the transient, the local heat transfer downstream of the prism is significantly modified as long as the obstacle is sufficiently close to the wall ($G/D \leqslant 0.1$) When the obstacle is attached to the wall ($G/D = 0$), one may observe up to 30% increase in local heat transfer whereas up to about 15% decrease is noted for the obstacle slightly detached from the wall ($G/D = 0.1$). For larger gap heights such that

$G/D \geqslant 0.15$, no significant influence on the local heat transfer is observed downstream of the prism. For this latter case, this is certainly due to the absence of a near-wake past the prism.

3. For small gap heights ($G/D \leqslant 0.1$) one observes as well enhancement ($G/D = 0$) as degradation ($G/D = 0.1$) in the heat transfer performance. The more marked phenomena occur in the early start-up of the free convection flow.
4. Upstream of the prism, the gap height has no influence on the heat transfer. Nevertheless, when the prism is at the wall ($G/D = 0$), this results in an important heat transfer degradation, up to 35%.

z

Acknowledgment

The authors gratefully acknowledge the research grant from the French Program "Amélioration des Echanges Thermiques".

References

Abu-Mulaweh, H.I., Armaly, B.F., Chen, T.S., 1995. Laminar natural convection flow over a vertical backward-facing step. J. Heat Transfer 117, 895–901.

Acharya, S., Mehrotra, A., 1993. Natural convection heat transfer in smooth and ribbed vertical channels. Int. J. Heat Mass Transfer 36, 236–241.

Aydin, M., 1997. Dependence of the natural convection over a vertical flat plate in the presence of the ribs. Int. Comm. Heat Mass Transfer 24, 521–531.

Bhavnani, S.H., Bergles, A.E., 1990. Effect of surface geometry and orientation on laminar natural convection heat transfer from a vertical flat plate with transverse roughness elements. Int. J. Heat Mass Transfer 33, 965–981.

Burak, V.S., Volkov, S.V., Martynenko, O.G., Khramtsov, P.P., Shikh, I.A., 1995. Experimental study of free-convective flow on a vertical plate with a constant heat flux in the presence of one or more steps. Int. J. Heat Mass Transfer 38, 147–154.

Desrayaud, G., Fichera, A., 2002. Laminar natural convection in a vertical isothermal channel with symmetric surface-mounted rectangular ribs. Int. J. Heat Fluid Flow 23, 519–529.

Hunt, J.C.R., Abell, C.J., Peterka, J.A., Woo, H., 1978. Kinematical studies of the flows around free or surface-mounted obstacles;applying topology to flow visualization. J. Fluid Mech. 86, 179–200.

Joshi, Y., Willson, T., Hazard, S.J., 1989. An experimental study of natural convection from an array of heated protrusions on a vertical surface in water. J. Electronic Packaging 111, 121–128.

Kakaç, S., Yener, Y., 1995. Convective Heat Transfer, second ed. CRC Press, Boca Raton.

Lin, T.Y., Hsieh, S.S., 1990. Natural convection of opposing/assisting flows in vertical channels with asymmetrically discrete heated ribs. Int. J. Heat Mass Transfer 33, 2295–2309.

Mladin, E.C., Polidori, G., de Lorenzo, T., 1999. Revisited laminar free convection theory by integral method. In: 9th Applied Thermodynamics National Conference, Craiova, Proceed., vol. II, pp. 227–238.

Polidori, G., Mladin, E.C., de Lorenzo, T., 2000. Extension de la méthode de Karman-Pohlhausen aux régimes transitoires de convection libre, pour $Pr > 0.6$. C. R. Acad. Sci. Paris 328, 763–766.

Polidori, G., Texier, O., Padet, J., 2002. Flow features and heat transfer in the separation region of obstacles in a transient free boundary layer. In: 12th Int. Heat Transfer Conference, Grenoble, Proceed., pp. 759–764.

Polidori, G., Padet, J., 2003. Transient free convection flow on a vertical surface with an array of large scale roughness elements. Exp. Thermal Fluid Sci. 27, 251–260.

Price, S.J., Sumner, D., Smith, J.G., Leong, K., Païdoussis, M.P., 2002. Flow visualization around a circular cylinder near to a plane wall. J. Fluids Struct. 16 (2), 175–191.

Rampanarivo, F., 2000. Etude du transfert convectif au sein d'une couche limite turbulente perturbée par un obstacle décollé de la paroi, Thèse Université de Valenciennes, France.

Shakerin, S., Bohn, M., Loehrke, R.I., 1988. Natural convection in an enclosure with discrete roughness elements on a vertical heated wall. Int. J. Heat Mass Transfer 31, 1423–1430.

Tanda, G., 1997. Natural convection heat transfer in vertical channels with and without transverse square ribs. Int. J. Heat Mass Transfer 40, 2173–2178.

Tsuji, T., Nagano, Y., 1988a. Characteristics of a turbulent natural convection boundary layer along a vertical flat plate. Int. J. Heat Mass Transfer 31, 1723–1734.

Tsuji, T., Nagano, Y., 1988b. Turbulence measurements in a natural convection boundary layer along a vertical flat plate. Int. J. Heat Mass Transfer 31, 2101–2111.

Tsuji, T., Nagano, Y., 1989. Velocity and temperature measurements in a natural convection boundary layer along a vertical flat plate. Exp. Thermal Fluid Sci. 2, 208–215.

Vermeulen, J.P., 1997. Etude de l'influence d'un obstacle sur le transfert thermique convectif en convection naturelle. Thèse Université de Valenciennes, France.

Vliet, G.C., Liu, C.K., 1969. An experimental study of turbulent natural convection boundary layer. J. Heat Transfer 91, 517–531.